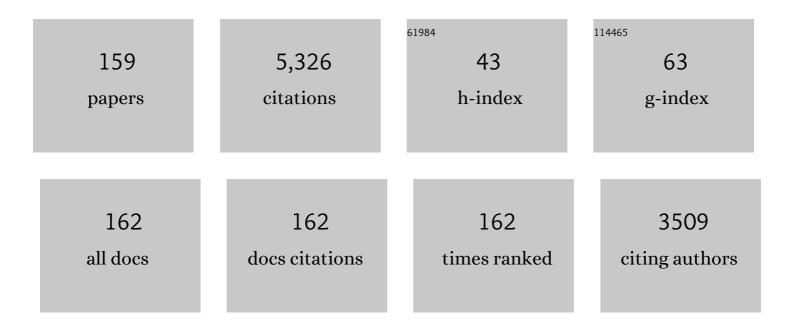
List of Publications by Year in descending order

Source: https://exaly.com/author-pdf/7707415/publications.pdf Version: 2024-02-01



#	Article	IF	CITATIONS
1	Changes in soil organic carbon and other physical soil properties along adjacent Mediterranean forest, grassland, and cropland ecosystems in Turkey. Journal of Arid Environments, 2004, 59, 743-752.	2.4	174
2	Pyrolytic kinetics, reaction mechanisms and products of waste tea via TG-FTIR and Py-GC/MS. Energy Conversion and Management, 2019, 184, 436-447.	9.2	173
3	Combustion behaviors of spent mushroom substrate using TG-MS and TG-FTIR: Thermal conversion, kinetic, thermodynamic and emission analyses. Bioresource Technology, 2018, 266, 389-397.	9.6	161
4	Pyrolysis of water hyacinth biomass parts: Bioenergy, gas emissions, and by-products using TG-FTIR and Py-GC/MS analyses. Energy Conversion and Management, 2020, 207, 112552.	9.2	150
5	Co-combustion thermal conversion characteristics of textile dyeing sludge and pomelo peel using TGA and artificial neural networks. Applied Energy, 2018, 212, 786-795.	10.1	132
6	TG-FTIR and Py-GC/MS analyses of pyrolysis behaviors and products of cattle manure in CO2 and N2 atmospheres: Kinetic, thermodynamic, and machine-learning models. Energy Conversion and Management, 2019, 195, 346-359.	9.2	124
7	Assessing the potential of renewable energy sources in Turkey. Renewable Energy, 2003, 28, 2303-2315.	8.9	114
8	Co-pyrolytic mechanisms, kinetics, emissions and products of biomass and sewage sludge in N2, CO2 and mixed atmospheres. Chemical Engineering Journal, 2020, 397, 125372.	12.7	103
9	Influence of catalysts on co-combustion of sewage sludge and water hyacinth blends as determined by TG-MS analysis. Bioresource Technology, 2018, 247, 217-225.	9.6	92
10	Pyrolysis dynamics of two medical plastic wastes: Drivers, behaviors, evolved gases, reaction mechanisms, and pathways. Journal of Hazardous Materials, 2021, 402, 123472.	12.4	92
11	Co-combustion of textile dyeing sludge with cattle manure: Assessment of thermal behavior, gaseous products, and ash characteristics. Journal of Cleaner Production, 2020, 253, 119950.	9.3	91
12	Dynamic pyrolysis behaviors, products, and mechanisms of waste rubber and polyurethane bicycle tires. Journal of Hazardous Materials, 2021, 402, 123516.	12.4	90
13	Combustion behaviors of three bamboo residues: Gas emission, kinetic, reaction mechanism and optimization patterns. Journal of Cleaner Production, 2019, 235, 549-561.	9.3	85
14	Environmental Monitoring of Land-Use and Land-Cover Changes in a Mediterranean Region of Turkey. Environmental Monitoring and Assessment, 2006, 114, 157-168.	2.7	82
15	Co-combustion of sewage sludge and coffee grounds under increased O2/CO2 atmospheres: Thermodynamic characteristics, kinetics and artificial neural network modeling. Bioresource Technology, 2018, 250, 230-238.	9.6	80
16	Ground-Based Optical Measurements at European Flux Sites: A Review of Methods, Instruments and Current Controversies. Sensors, 2011, 11, 7954-7981.	3.8	76
17	Thermal degradations and processes of waste tea and tea leaves via TG-FTIR: Combustion performances, kinetics, thermodynamics, products and optimization. Bioresource Technology, 2018, 268, 715-725.	9.6	75
18	Co-pyrolytic performances, mechanisms, gases, oils, and chars of textile dyeing sludge and waste shared bike tires under varying conditions. Chemical Engineering Journal, 2022, 428, 131053.	12.7	75

#	Article	IF	CITATIONS
19	Comparative (co-)pyrolytic performances and by-products of textile dyeing sludge and cattle manure: Deeper insights from Py-GC/MS, TG-FTIR, 2D-COS and PCA analyses. Journal of Hazardous Materials, 2021, 401, 123276.	12.4	70
20	Comparative thermogravimetric analyses of co-combustion of textile dyeing sludge and sugarcane bagasse in carbon dioxide/oxygen and nitrogen/oxygen atmospheres: Thermal conversion characteristics, kinetics, and thermodynamics. Bioresource Technology, 2018, 255, 88-95.	9.6	69
21	Combustions of torrefaction-pretreated bamboo forest residues: Physicochemical properties, evolved gases, and kinetic mechanisms. Bioresource Technology, 2020, 304, 122960.	9.6	69
22	Ground-Based Optical Measurements at European Flux Sites: A Review of Methods, Instruments and Current Controversies. Sensors, 2011, 11, 7954-7981.	3.8	67
23	Combustion behaviors of pileus and stipe parts of Lentinus edodes using thermogravimetric-mass spectrometry and Fourier transform infrared spectroscopy analyses: Thermal conversion, kinetic, thermodynamic, gas emission and optimization analyses. Bioresource Technology, 2019, 288, 121481.	9.6	67
24	Interaction effects of chlorine and phosphorus on thermochemical behaviors of heavy metals during incineration of sulfur-rich textile dyeing sludge. Chemical Engineering Journal, 2018, 351, 897-911.	12.7	65
25	Thermal characteristics, kinetics, gas emissions and thermodynamic simulations of (co-)combustions of textile dyeing sludge and waste tea. Journal of Cleaner Production, 2019, 239, 118113.	9.3	65
26	Synergistic effects, gaseous products, and evolutions of NOx precursors during (co-)pyrolysis of textile dyeing sludge and bamboo residues. Journal of Hazardous Materials, 2021, 401, 123331.	12.4	65
27	Spatio-temporal modeling of global solar radiation dynamics as a function of sunshine duration for Turkey. Agricultural and Forest Meteorology, 2007, 145, 36-47.	4.8	61
28	(Co-)combustion behaviors and products of spent potlining and textile dyeing sludge. Journal of Cleaner Production, 2019, 224, 384-395.	9.3	61
29	Kinetics, thermodynamics, gas evolution and empirical optimization of cattle manure combustion in air and oxy-fuel atmospheres. Applied Thermal Engineering, 2019, 149, 119-131.	6.0	60
30	Catalytic effects of CaO, Al2O3, Fe2O3, and red mud on Pteris vittata combustion: Emission, kinetic and ash conversion patterns. Journal of Cleaner Production, 2020, 252, 119646.	9.3	60
31	Thermogravimetric analysis of (co-)combustion of oily sludge and litchi peels: combustion characterization, interactions and kinetics. Thermochimica Acta, 2018, 667, 207-218.	2.7	59
32	Flue gas-to-ash desulfurization of combustion of textile dyeing sludge: Its dependency on temperature, lignocellulosic residue, and CaO. Chemical Engineering Journal, 2021, 417, 127906.	12.7	58
33	Coastal Flood Risk Analysis Using Landsat-7 ETM+ Imagery and SRTM DEM: A Case Study of Izmir, Turkey. Environmental Monitoring and Assessment, 2007, 131, 293-300.	2.7	56
34	Co-pyrolysis performances, synergistic mechanisms, and products of textile dyeing sludge and medical plastic wastes. Science of the Total Environment, 2021, 799, 149397.	8.0	56
35	Thermal conversion behaviors and products of spent mushroom substrate in CO2 and N2 atmospheres: Kinetic, thermodynamic, TG and Py-GC/MS analyses. Journal of Analytical and Applied Pyrolysis, 2019, 139, 177-186.	5.5	55
36	Co-combustion, life-cycle circularity, and artificial intelligence-based multi-objective optimization of two plastics and textile dyeing sludge. Journal of Hazardous Materials, 2022, 426, 128069.	12.4	53

#	Article	IF	CITATIONS
37	Assessing thermal behaviors and kinetics of (co-)combustion of textile dyeing sludge and sugarcane bagasse. Applied Thermal Engineering, 2018, 131, 874-883.	6.0	50
38	Kinetics, thermodynamics, gas evolution and empirical optimization of (co-)combustion performances of spent mushroom substrate and textile dyeing sludge. Bioresource Technology, 2019, 280, 313-324.	9.6	50
39	Bioenergy and emission characterizations of catalytic combustion and pyrolysis of litchi peels via TG-FTIR-MS and Py-GC/MS. Renewable Energy, 2020, 148, 1074-1093.	8.9	50
40	Combustion behaviors of Pteris vittata using thermogravimetric, kinetic, emission and optimization analyses. Journal of Cleaner Production, 2019, 237, 117772.	9.3	49
41	Pyrolysis performance, kinetic, thermodynamic, product and joint optimization analyses of incense sticks in N2 and CO2 atmospheres. Renewable Energy, 2019, 141, 814-827.	8.9	48
42	Oxy-fuel and air atmosphere combustions of Chinese medicine residues: Performances, mechanisms, flue gas emission, and ash properties. Renewable Energy, 2022, 182, 102-118.	8.9	47
43	Quantifying thermal decomposition regimes of textile dyeing sludge, pomelo peel, and their blends. Renewable Energy, 2018, 122, 55-64.	8.9	46
44	Torrefaction, temperature, and heating rate dependencies of pyrolysis of coffee grounds: Its performances, bio-oils, and emissions. Bioresource Technology, 2022, 345, 126346.	9.6	46
45	CO2-assisted co-pyrolysis of textile dyeing sludge and hyperaccumulator biomass: Dynamic and comparative analyses of evolved gases, bio-oils, biochars, and reaction mechanisms. Journal of Hazardous Materials, 2020, 400, 123190.	12.4	45
46	Pyrolytic behaviors, kinetics, decomposition mechanisms, product distributions and joint optimization of Lentinus edodes stipe. Energy Conversion and Management, 2020, 213, 112858.	9.2	43
47	Quantifying coastal inundation vulnerability of Turkey to sea-level rise. Environmental Monitoring and Assessment, 2008, 138, 101-106.	2.7	41
48	Delving deeper: Metabolic processes in the metalimnion of stratified lakes. Limnology and Oceanography, 2017, 62, 1288-1306.	3.1	40
49	Assessing Major Ecosystem Types and the Challenge of Sustainability in Turkey. Environmental Management, 2000, 26, 479-489.	2.7	38
50	Deriving Vegetation Dynamics of Natural Terrestrial Ecosystems from MODIS NDVI/EVI Data over Turkey. Sensors, 2008, 8, 5270-5302.	3.8	37
51	Thermogravimetric and mass-spectrometric analyses of combustion of spent potlining under N2/O2 and CO2/O2 atmospheres. Waste Management, 2019, 87, 237-249.	7.4	37
52	Evaluation of reaction mechanisms and emissions of oily sludge and coal co-combustions in O2/CO2 and O2/N2 atmospheres. Renewable Energy, 2021, 171, 1327-1343.	8.9	37
53	(Co-)combustion of additives, water hyacinth and sewage sludge: Thermogravimetric, kinetic, gas and thermodynamic modeling analyses. Waste Management, 2018, 81, 211-219.	7.4	36
54	(Co-)pyrolytic performances and by-products of textile dyeing sludge and spent mushroom substrate. Journal of Cleaner Production, 2020, 261, 121195.	9.3	36

#	Article	IF	CITATIONS
55	Oxy-fuel co-combustion dynamics of phytoremediation biomass and textile dyeing sludge: Gas-to-ash pollution abatement. Science of the Total Environment, 2022, 825, 153656.	8.0	36
56	Efficiency, by-product valorization, and pollution control of co-pyrolysis of textile dyeing sludge and waste solid adsorbents: Their atmosphere, temperature, and blend ratio dependencies. Science of the Total Environment, 2022, 819, 152923.	8.0	35
57	Emission-to-ash detoxification mechanisms of co-combustion of spent pot lining and pulverized coal. Journal of Hazardous Materials, 2021, 418, 126380.	12.4	33
58	Modeling Spatio-Temporal Dynamics of Optimum Tilt Angles for Solar Collectors in Turkey. Sensors, 2008, 8, 2913-2931.	3.8	32
59	Optimizing bioenergy and by-product outputs from durian shell pyrolysis. Renewable Energy, 2021, 164, 407-418.	8.9	32
60	Assessing solar radiation models using multiple variables over Turkey. Climate Dynamics, 2008, 31, 131-149.	3.8	31
61	The mixture of sewage sludge and biomass waste as solid biofuels: Process characteristic and environmental implication. Renewable Energy, 2019, 139, 707-717.	8.9	31
62	Co-pyrolytic mechanisms and products of textile dyeing sludge and durian shell in changing operational conditions. Chemical Engineering Journal, 2021, 420, 129711.	12.7	30
63	Torrefaction-assisted oxy-fuel co-combustion of textile dyeing sludge and bamboo residues toward enhancing emission-to-ash desulfurization in full waste circularity. Fuel, 2022, 318, 123603.	6.4	30
64	Changing Global Climate: Historical Carbon and Nitrogen Budgets and Projected Responses of Ohio?s Cropland Ecosystems. Ecosystems, 2004, 7, 381.	3.4	29
65	Quantifying Carbon Budgets Of Conifer Mediterranean Forest Ecosystems, Turkey. Environmental Monitoring and Assessment, 2006, 119, 527-543.	2.7	29
66	Large interannual variability in net ecosystem carbon dioxide exchange of a disturbed temperate peatland. Science of the Total Environment, 2016, 554-555, 192-202.	8.0	27
67	Oxy-fuel and air combustion performances and gas-to-ash products of aboveground and belowground biomass of Sedum alfredii Hance. Chemical Engineering Journal, 2021, 422, 130312.	12.7	27
68	Ash-to-emission pollution controls on co-combustion of textile dyeing sludge and waste tea. Science of the Total Environment, 2021, 794, 148667.	8.0	27
69	Water quality time series for Big Melen stream (Turkey): its decomposition analysis and comparison to upstream. Environmental Monitoring and Assessment, 2010, 165, 125-136.	2.7	26
70	Response surface optimization, modeling and uncertainty analysis of mass loss response of co-combustion of sewage sludge and water hyacinth. Applied Thermal Engineering, 2017, 125, 328-335.	6.0	26
71	Characterizing and optimizing (co-)pyrolysis as a function of different feedstocks, atmospheres, blend ratios, and heating rates. Bioresource Technology, 2019, 277, 104-116.	9.6	26
72	Catalytic combustion performances, kinetics, reaction mechanisms and gas emissions of Lentinus edodes. Bioresource Technology, 2020, 300, 122630.	9.6	26

#	Article	IF	CITATIONS
73	Bottom slag-to-flue gas controls on S and Cl from co-combustion of textile dyeing sludge and waste biochar: Their interactions with temperature, atmosphere, and blend ratio. Journal of Hazardous Materials, 2022, 435, 129007.	12.4	26
74	Modeling Forest Productivity Using Envisat MERIS Data. Sensors, 2007, 7, 2115-2127.	3.8	25
75	Uncertainty and sensitivity analyses of co-combustion/pyrolysis of textile dyeing sludge and incense sticks: Regression and machine-learning models. Renewable Energy, 2020, 151, 463-474.	8.9	25
76	Catalytic combustions of two bamboo residues with sludge ash, CaO, and Fe2O3: Bioenergy, emission and ash deposition improvements. Journal of Cleaner Production, 2020, 270, 122418.	9.3	25
77	Modelling stochastic variability and uncertainty in aroma active compounds of PEF-treated peach nectar as a function of physical and sensory properties, and treatment time. Food Chemistry, 2016, 190, 634-642.	8.2	24
78	Modelling long-term C dynamics in croplands in the context of climate change: a case study from Ohio. Environmental Modelling and Software, 2001, 16, 361-375.	4.5	23
79	Optimizing environmental pollution controls in response to textile dyeing sludge, incineration temperature, CaO conditioner, and ash minerals. Science of the Total Environment, 2021, 785, 147219.	8.0	23
80	Monitoring Water Quality and Quantity of National Watersheds in Turkey. Environmental Monitoring and Assessment, 2007, 133, 215-229.	2.7	22
81	Implications of climate change for evaporation from bare soils in a Mediterranean environment. Environmental Monitoring and Assessment, 2008, 140, 123-130.	2.7	22
82	Combustion parameters, evolved gases, reaction mechanisms, and ash mineral behaviors of durian shells: A comprehensive characterization and joint-optimization. Bioresource Technology, 2020, 314, 123689.	9.6	22
83	Thermal behaviors of fluorine during (co-)incinerations of spent potlining and red mud: Transformation, retention, leaching and thermodynamic modeling analyses. Chemosphere, 2020, 249, 126204.	8.2	22
84	Developing a suitability index for land uses and agricultural land covers: A case study in Turkey. Environmental Monitoring and Assessment, 2005, 102, 323-335.	2.7	21
85	Performance and mechanism of bamboo residues pyrolysis: Gas emissions, by-products, and reaction kinetics. Science of the Total Environment, 2022, 838, 156560.	8.0	21
86	Techno-Economic Analysis of Solar Water Heating Systems inTurkey. Sensors, 2008, 8, 1252-1277.	3.8	20
87	Historical spatiotemporal analysis of land-use/land-cover changes and carbon budget in a temperate peatland (Turkey) using remotely sensed data. Applied Geography, 2011, 31, 1166-1172.	3.7	20
88	Coupled mechanisms of reaction kinetics, gas emissions, and ash mineral transformations during combustion of AlCl3-conditioned textile dyeing sludge. Journal of Hazardous Materials, 2021, 403, 123968.	12.4	20
89	Quantifying rates and drivers of change in long-term sector- and country-specific trends of carbon dioxide-equivalent greenhouse gas emissions. Renewable and Sustainable Energy Reviews, 2016, 65, 823-831.	16.4	19
90	Turning the co-combustion synergy of textile dyeing sludge and waste biochar into emission-to-bottom slag pollution controls toward a circular economy. Renewable Energy, 2022, 194, 760-777.	8.9	19

#	Article	IF	CITATIONS
91	Agricultural sustainability in Turkey: integrating food, environmental and energy securities. Land Degradation and Development, 2002, 13, 61-67.	3.9	18
92	Assessing monthly average solar radiation models: a comparative case study in Turkey. Environmental Monitoring and Assessment, 2011, 175, 251-277.	2.7	18
93	Modeling Potential Distribution and Carbon Dynamics of Natural Terrestrial Ecosystems: A Case Study of Turkey. Sensors, 2007, 7, 2273-2296.	3.8	17
94	Assessing neural networks with wavelet denoising and regression models in predicting diel dynamics of eddy covariance-measured latent and sensible heat fluxes and evapotranspiration. Neural Computing and Applications, 2014, 24, 327-337.	5.6	17
95	Monitoring diel dissolved oxygen dynamics through integrating wavelet denoising and temporal neural networks. Environmental Monitoring and Assessment, 2014, 186, 1583-1591.	2.7	17
96	Statistical Modeling of Spatio-Temporal Variability in Monthly Average Daily Solar Radiation over Turkey. Sensors, 2007, 7, 2763-2778.	3.8	16
97	Spatial viability analysis of grid-connected photovoltaic power systems for Turkey. International Journal of Electrical Power and Energy Systems, 2014, 56, 270-278.	5.5	16
98	Dynamic insights into combustion drivers and responses of water hyacinth: Evolved gas and ash analyses. Journal of Cleaner Production, 2020, 276, 124156.	9.3	16
99	Reaction mechanisms and product patterns of Pteris vittata pyrolysis for cleaner energy. Renewable Energy, 2021, 167, 600-612.	8.9	16
100	Quantifying spatio-temporal dynamics of solar radiation exergy over Turkey. Renewable Energy, 2010, 35, 2821-2828.	8.9	15
101	Monitoring and validating spatio-temporal dynamics of biogeochemical properties in Mersin Bay (Turkey) using Landsat ETM+. Environmental Monitoring and Assessment, 2011, 181, 457-464.	2.7	14
102	Regression model-based predictions of diel, diurnal and nocturnal dissolved oxygen dynamics after wavelet denoising of noisy time series. Physica A: Statistical Mechanics and Its Applications, 2014, 404, 8-15.	2.6	14
103	Water-soluble fluorine detoxification mechanisms of spent potlining incineration in response to calcium compounds. Environmental Pollution, 2020, 266, 115420.	7.5	14
104	Dynamic pyrolytic reaction mechanisms, pathways, and products of medical masks and infusion tubes. Science of the Total Environment, 2022, 842, 156710.	8.0	14
105	Quantifying spatial patterns of bioclimatic zones and controls in Turkey. Theoretical and Applied Climatology, 2008, 91, 35-50.	2.8	13
106	Boosted decision tree classifications of land cover over Turkey integrating MODIS, climate and topographic data. International Journal of Remote Sensing, 2011, 32, 3461-3483.	2.9	13
107	Satellite-based and mesoscale regression modeling of monthly air and soil temperatures over complex terrain in Turkey. Expert Systems With Applications, 2012, 39, 2059-2066.	7.6	13
108	Multiple drivers, interaction effects, and trade-offs of efficient and cleaner combustion of torrefied water hyacinth. Science of the Total Environment, 2021, 786, 147278.	8.0	13

#	Article	IF	CITATIONS
109	Yield and Fruit Quality of Watermelon (<i>Citrullus lanatus</i> (Thumb.) Matsum. & Nakai.) and Melon (<i>Cucumis melo</i> L.) under Protected Organic and Conventional Farming Systems in a Mediterranean Region of Turkey. Biological Agriculture and Horticulture, 2004, 22, 173-183.	1.0	12
110	Spatial and temporal variations in diurnal CO2fluxes of different Mediterranean ecosystems in Turkey. Journal of Environmental Monitoring, 2005, 7, 151-157.	2.1	12
111	Quantifying long-term changes in water quality and quantity of Euphrates and Tigris rivers, Turkey. Environmental Monitoring and Assessment, 2010, 170, 475-490.	2.7	12
112	An inventory-based carbon budget for forest and woodland ecosystems of Turkey. Journal of Environmental Monitoring, 2004, 6, 26.	2.1	11
113	Quantifying soil respiration in response to short-term tillage practices: a case study in southern Turkey. Acta Agriculturae Scandinavica - Section B Soil and Plant Science, 2009, 59, 50-56.	0.6	11
114	Predicting Diel, Diurnal and Nocturnal Dynamics of Dissolved Oxygen and Chlorophyllâ€ <i>a</i> Using Regression Models and Neural Networks. Clean - Soil, Air, Water, 2013, 41, 872-877.	1.1	11
115	Quantifying biosphere–atmosphere exchange of CO2 using eddy covariance, wavelet denoising, neural networks, and multiple regression models. Agricultural and Forest Meteorology, 2013, 171-172, 1-8.	4.8	9
116	Spatiotemporal modeling of saturated dissolved oxygen through regressions after wavelet denoising of remotely and proximally sensed data. Earth Science Informatics, 2015, 8, 247-254.	3.2	9
117	Thermodynamic behaviors of Cu in interaction with chlorine, sulfur, phosphorus and minerals during sewage sludge co-incineration. Chinese Journal of Chemical Engineering, 2018, 26, 1160-1170.	3.5	9
118	Parametric assessment of stochastic variability in co-combustion of textile dyeing sludge and shaddock peel. Waste Management, 2019, 96, 128-135.	7.4	9
119	Arsenic Partitioning Behavior During Sludge Co-combustion: Thermodynamic Equilibrium Simulation. Waste and Biomass Valorization, 2019, 10, 2297-2307.	3.4	9
120	Falling Dynamics of SARS-CoV-2 as a Function of Respiratory Droplet Size and Human Height. Journal of Medical and Biological Engineering, 2020, 40, 880-886.	1.8	9
121	Technical and environmental feasibility of gas-solid decontamination by oxygen-enriched co-combustion of textile dyeing sludge and durian shell. Journal of Cleaner Production, 2022, 360, 131967.	9.3	9
122	Modeling aboveâ€ground litterfall in eastern Mediterranean conifer forests using fractional tree cover, and remotely sensed and ground data. Applied Vegetation Science, 2010, 13, 485-497.	1.9	8
123	Assessing CO ₂ sink/source strength of a degraded temperate peatland: atmospheric and hydrological drivers and responses to extreme events. Ecohydrology, 2015, 8, 1429-1445.	2.4	8
124	Spatiotemporal modeling of watershed nutrient transport dynamics: Implications for eutrophication abatement. Ecological Informatics, 2016, 34, 52-69.	5.2	8
125	Compositing climate change vulnerability of a Mediterranean region using spatiotemporally dynamic proxies for ecological and socioeconomic impacts and stabilities. Environmental Monitoring and Assessment, 2017, 189, 29.	2.7	8
126	Using Eddy Covariance Sensors to Quantify Carbon Metabolism of Peatlands: A Case Study in Turkey. Sensors, 2011, 11, 522-538.	3.8	7

#	Article	IF	CITATIONS
127	Thermochemical behaviorsof textile dying sludge, paper mill sludge, and their blends during (co-)combustion. Thermochimica Acta, 2017, 655, 101-105.	2.7	7
128	Modeling and Validating Longâ€Term Dynamics of Diel Dissolved Oxygen with Particular Reference to pH in a Temperate Shallow Lake (Turkey). Clean - Soil, Air, Water, 2011, 39, 966-971.	1.1	6
129	Multivariate analysis of watershed health and sustainability in Turkey. International Journal of Sustainable Development and World Ecology, 2008, 15, 265-272.	5.9	5
130	Modeling Net Ecosystem Carbon Dioxide Exchange Using Temporal Neural Networks after Wavelet Denoising. Geographical Analysis, 2014, 46, 37-52.	3.5	5
131	Thermodynamic equilibrium predictions of zinc volatilization, migration, and transformation during sludge coâ€incineration. Water Environment Research, 2019, 91, 208-221.	2.7	5
132	Monitoring spatiotemporal variations of diel radon concentrations in peatland and forest ecosystems based on neural network and regression models. Environmental Monitoring and Assessment, 2013, 185, 5577-5583.	2.7	4
133	How Do Different Locations, Floors and Aspects Influence Indoor Radon Concentrations? An Empirical Study Using Neural Networks for a University Campus in Northwestern Turkey. Indoor and Built Environment, 2013, 22, 650-658.	2.8	4
134	Coupling of remote sensing, field campaign, and mechanistic and empirical modeling to monitor spatiotemporal carbon dynamics of a Mediterranean watershed in a changing regional climate. Environmental Monitoring and Assessment, 2015, 187, 179.	2.7	4
135	Long-term spatiotemporal patterns of CH4 and N2O emissions from livestock and poultry production in Turkey. Environmental Monitoring and Assessment, 2010, 167, 545-558.	2.7	3
136	Quantifying Environmental Flow Requirement Towards Watershed Sustainability. Asian Journal of Chemistry, 2013, 25, 2622-2626.	0.3	3
137	Thermodynamic Equilibrium Simulations of ThalliumÂDistributions in Interactions with Chlorine, Sulfur, Phosphorus, and Minerals During Sludge Co-combustion. Waste and Biomass Valorization, 2020, 11, 1251-1259.	3.4	3
138	Modeling Impacts of Land Uses on Carbon and Nitrogen Contents, Carbon Dioxide and Water Effluxes of Mediterranean Soils. Polish Journal of Environmental Studies, 2016, 25, 1479-1487.	1.2	3
139	NOVEL USES OF RED MUD IN TEXTILE WASTEWATER TREATMENT, DYEING, AND CONCRETE PRODUCTION. Environmental Engineering and Management Journal, 2015, 14, 1171-1181.	0.6	3
140	Data-driven simulations of flank wear of coated cutting tools in hard turning. Mechanika, 2016, 21, .	0.5	3
141	Diurnal photosynthesis, water use efficiency and light use efficiency of wheat under Mediterranean field conditions. Journal of Environmental Biology, 2008, 29, 397-406.	0.5	3
142	Effects of Strip Intercropping and Organic Farming Systems on Quantity and Quality of Maize Yield in a Mediterranean Region of Turkey. Agroecology and Sustainable Food Systems, 2007, 30, 109-118.	0.9	2
143	Modeling Efficiency of Dehydrated Sunflower Seed Cake as a Novel Biosorbent to Remove a Toxic Azo Dye. Chemical Engineering Communications, 2015, , 151007222219007.	2.6	2
144	Utilizing aluminum etching wastewater for tannery wastewater coagulation: performance and feasibility. Desalination and Water Treatment, 2016, 57, 2413-2421.	1.0	2

#	Article	IF	CITATIONS
145	Estimating Spatio-temporal Responses of Net Primary Productivity to Climate Change Scenarios in the Seyhan Watershed by Integrating Biogeochemical Modelling and Remote Sensing. The Anthropocene: Politik - Economics - Society - Science, 2019, , 183-199.	0.2	2
146	Juxtaposing the spatiotemporal drivers of sediment CO2, CH4, and N2O effluxes along ecoregional, wet-dry, and diurnal gradients. Atmospheric Pollution Research, 2021, 12, 160-171.	3.8	2
147	A model for indoor motion dynamics of SARS-CoV-2 as a function of respiratory droplet size and evaporation. Environmental Monitoring and Assessment, 2021, 193, 626.	2.7	2
148	Ultrasound–assisted adsorption of toxic dyes by cottonseed cake: artificial neural networks, regression models and response surface optimization. Global Nest Journal, 2018, 20, 14-24.	0.1	2
149	Handheld two-stroke engines as an important source of personal VOC exposure for olive farm workers. Environmental Science and Pollution Research, 0, , .	5.3	2
150	Integrating Map Algebra and Statistical Modeling for Spatio- Temporal Analysis of Monthly Mean Daily Incident Photosynthetically Active Radiation (PAR) over a Complex Terrain. Sensors, 2007, 7, 3242-3257.	3.8	1
151	Modeling Ultrasound-Assisted Decolorization Efficiency of Reactive Red 195 Using Soybean Cake. Asian Journal of Chemistry, 2015, 27, 4541-4548.	0.3	1
152	Integrating spatiotemporal dynamics of natural capital security and urban ecosystem carbon metabolism. Environment, Development and Sustainability, 2018, 20, 2043-2063.	5.0	1
153	Interaction effects of the main drivers of global climate change on spatiotemporal dynamics of high altitude ecosystem behaviors: process-based modeling. Environmental Monitoring and Assessment, 2020, 192, 457.	2.7	1
154	EMISSIONS OF GREENHOUSE GASES FROM DIESEL CONSUMPTION IN AGRICULTURAL PRODUCTION OF TURKEY. European Journal of Sustainable Development (discontinued), 2016, 5, .	0.9	1
155	Multivariate empirical modeling of interaction effects of machining var-iables on surface roughness in dry hard turning of AISI 4140 steel with coated CBN insert using Taguchi design. Mechanika, 2017, 23,	0.5	1
156	Identification of ecologically significant habitats for urban nature conservation: a case study in Turkey. Journal of Environmental Biology, 2003, 24, 241-51.	0.5	1
157	Dynamic Emulations of Surface Radiation Components During Day and Night Under all Sky and Surface Conditions Using Temporal Neural Networks. International Journal of Green Energy, 2013, 10, 966-983.	3.8	0
158	Quantifying spatiotemporal rhythm of stream metabolism along human disturbance gradients. Annales De Limnologie, 2020, 56, 16.	0.6	0
159	Transport dynamics of SARS-CoV-2 under outdoor conditions. Air Quality, Atmosphere and Health, 2022, , 1-7.	3.3	0